



Liquid-like Poly(ionic liquid) as Electrolyte for Thermally Stable Lithium-Ion Battery

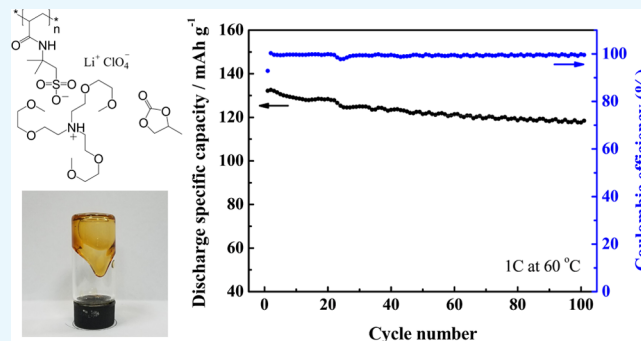
Zhiyun Zhang,[†] Yelong Zhang,[‡] Binyang Du,^{*,†,ID} and Zhangquan Peng^{*,‡,ID}

[†]MOE Key Laboratory of Macromolecular Synthesis and Functionalization, Department of Polymer Science & Engineering, Zhejiang University, Hangzhou 310027, China

[‡]Changchun Institute of Applied Chemistry, Chinese Academy of Sciences, Changchun 130022, China

Supporting Information

ABSTRACT: A liquid-like poly(ionic liquid) (PIL) with a very low glass transition temperature of -51°C and a thermal decomposition temperature of 202.7°C was synthesized. A PIL-based electrolyte by mixing this poly(ionic liquid) with additives of 10 wt % propylene carbonate and 0.1 M LiClO₄ is proved to be an excellent electrolyte for lithium-ion battery. The obtained PIL-based electrolyte exhibits a high ionic conductivity of $8.3 \times 10^{-5} \text{ S cm}^{-1}$ at 25°C and $2.0 \times 10^{-4} \text{ S cm}^{-1}$ at 60°C and a wide electrochemical potential window up to 5.61 V at 25°C and 4.14 V at 60°C . The Li/LiFePO₄ batteries equipped with this PIL-based electrolyte achieve high capacity, outstanding cycling stability and rate capability at 25°C , and even improved performance at high temperature like 60°C . Such excellent performances of batteries are attributed to the formation of stable solid-electrolyte interface film at the lithium-electrolyte interface and the stability of electrolyte during cycling.



1. INTRODUCTION

Lithium-ion batteries (LIBs) possess high specific capacities (for example, 170 mAh g^{-1} with LiFePO₄ (LFP) as cathode¹) and have been widely used in today's technological products such as smart phone, laptop computer, electric vehicles, and hybrid electric vehicles. Yet, safety problems in LIBs, especially in the electrolyte, are still important issues and further improvements are strongly desired. Traditionally, ethylene carbonate, propylene carbonate (PC), dimethyl carbonate, or their hybrid solvents are used as electrolytes because of the advantages like low cost, high conductivity, and low melting point.^{2–6} However, such electrolytes associate at the same time with several serious safety problems. For example, the low flashing point means that the electrolyte can catch fire easily in case of local overheating in the battery. The volatilization of the electrolyte in an airtight cell might cause the battery to expand, resulting in the leakage of electrolyte and hence the damage of the product.

Polymers have excellent thermal stability and are non-volatile. Therefore, they are applied as electrolytes to improve the safety of LIBs.^{7–9} The most commonly used polymers are poly(ethylene oxide) (PEO) and PEO-based polymers because the PEO chain segments are flexible and their $-\text{CH}_2\text{CH}_2\text{O}-$ repeat unit can provide good solubility and conductivity to Li⁺.¹⁰ However, PEO is not conductive and usually solid-like at room temperature, resulting in the low ionic conductivity of the electrolyte. Alternatively, room-temperature ionic liquids are also extensively investigated as electrolytes for enhancing

the safety of LIBs because the ionic liquids have high ionic conductivity, negligible volatility, and good thermal, chemical, and electrochemical stabilities.^{11–13} Advantages of both polymers and ionic liquids can be combined to give poly(ionic liquid)s (PILs), which can be designed and synthesized for some specific applications as gas adsorption materials, antimicrobial materials, catalytic materials, electrochemical energy materials, and the likes.^{14,15} Wang et al.¹⁶ reported a PIL, poly(*N*-(1-vinylimidazolium-3-butyl)-ammonium bis(trifluoromethanesulfonyl) imide)-co-poly(ethylene glycol) methyl ether methacrylate) (PVIMTFSI-*co*-PPEGMA), which can be used to fabricate all-solid electrolyte (PVIMTFSI-*co*-PPEGMA/LiTFSI) by mixing with lithium bis-(trifluoromethylsulfonyl)imide (LiTFSI). For the PVIMTFSI-*co*-PPEGMA/LiTFSI-based LiFePO₄/Li battery, the discharge-specific capacities of 136 and 70 mAh g^{-1} at current densities of 0.1 and 1C were achieved at 60°C , respectively. The authors also demonstrated that the polymeric ionic liquid segments can restrain the formation of lithium dendrites.¹⁶ Lu et al.¹⁷ constructed a PIL-based electrolyte film based on a lithium-containing zwitterionic poly(ionic liquid) (PIL) with or without propylene carbonate (PC) by *in situ* photopolymerization. The lithium-containing IL was synthesized by equimolecular neutralization of 3-(1-vinyl-3-imidazo-

Received: July 4, 2018

Accepted: August 21, 2018

Published: September 5, 2018



Scheme 1. Synthesis Routines of ATA and PATA

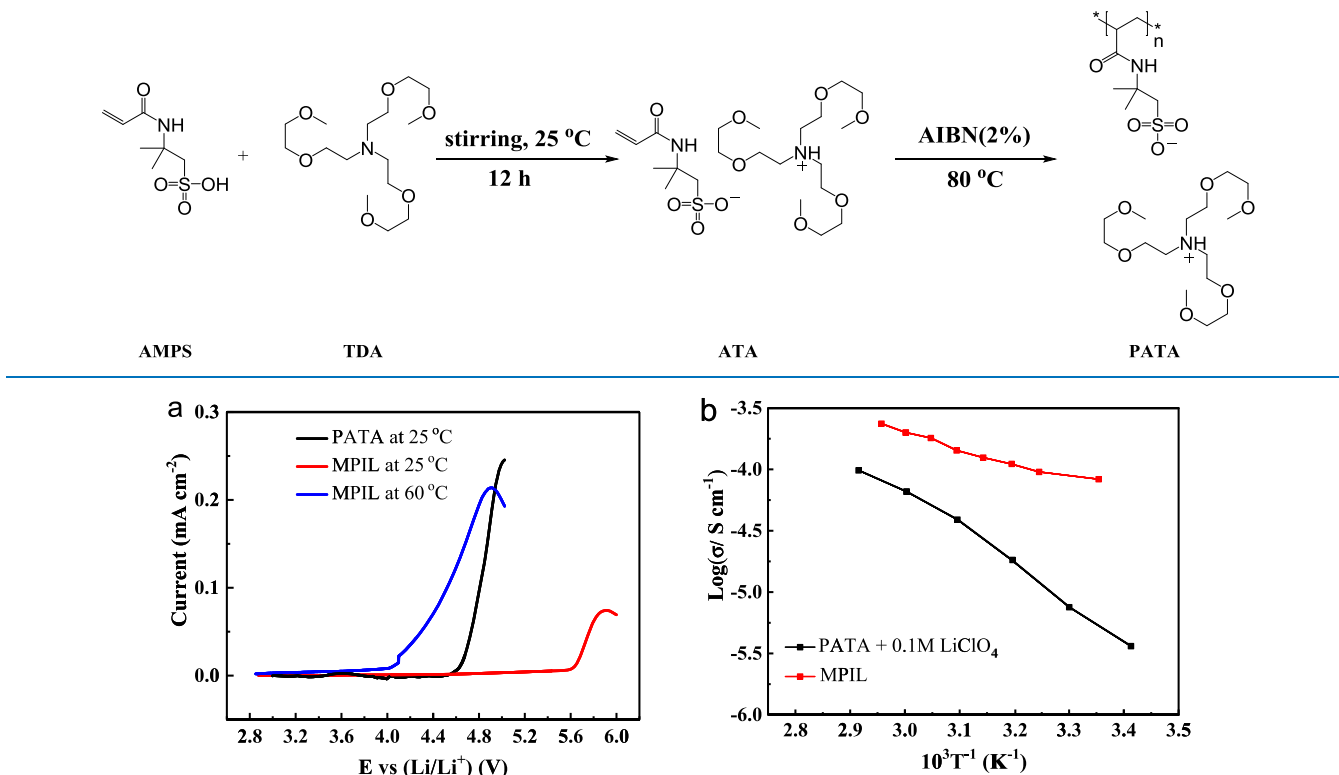


Figure 1. (a) Linear sweep voltammetry curves of PATA and MPIL at 25 °C as well as MPIL at 60 °C. (b) Temperature-dependent ionic conductivities of PATA with 0.1 M LiClO₄ and MPIL.

lio)-propanesulfonate and LiTFSI. With 50–90 wt % PC, a comparable ionic conductivity of $\sim 10^{-3}$ S cm⁻¹ was obtained for the PIL-based electrolyte film at 30 °C. The Li/LiFePO₄ half-cell equipped with the PIL/30PC film (30 wt % PC) shows a good initial discharge-specific capacity of 120.4 mAh g⁻¹, and the corresponding Coulombic efficiency is 89.1% at 0.1C. However, the discharge-specific capacity of the Li/LiFePO₄ half-cell decreases slowly with cycling to reach 99.2 mAh g⁻¹ in the 30th cycle, indicating the existence of irreversible electrochemical reactions of the electrode.¹⁷

However, most reported PILs are solid-like at room temperature, so their ionic conductivities are usually rather low at the temperature. The reports of room-temperature liquid-like PILs are rare.^{18,19} The liquid-like PILs might have improve ionic conductivity. Snow et al. reported the first example of liquid-like poly(ionic liquid), which showed a low glass transition temperature (T_g) of -47 °C and an electrowetting effect.¹⁸ Yuan et al. reported the second example of liquid-like poly(ionic liquid), which showed a low T_g of -57 °C and exhibited fluidic behavior in a wide temperature range from room temperature to its decomposition temperature, and explored its application as macromolecular solvent and reaction medium.¹⁹ However, the application of liquid-like PILs as electrolytes for LIBs has not yet been investigated. Herein, we shall report a novel PIL-based electrolyte, namely, MPIL, by mixing a liquid-like poly(ionic liquid) with additives of 10 wt % propylene carbonate (PC) and 0.1 M LiClO₄ for LIBs. The MPIL electrolyte exhibits a high ionic conductivity of 8.3×10^{-5} S cm⁻¹ at 25 °C and 2.0×10^{-4} S cm⁻¹ at 60 °C with a wide electrochemical potential window up to 5.61 V at 25 °C and

4.14 V at 60 °C, respectively. The Li/LiFePO₄ batteries with MPIL electrolyte show a reversible discharge-specific capacities of 137.4 and 110 mAh g⁻¹ at the current densities of 0.1 and 1C, respectively, for the first cycle at 25 °C, which are maintained at 127.4 and 116.3 mAh g⁻¹ after 100 cycles, respectively, with Coulombic efficiency of 100%. Furthermore, the batteries show improved performance at high temperature. The discharge-specific capacities of the batteries reach 144 and 126 mAh g⁻¹ at 0.1 and 1C, respectively, at 60 °C. The formation of a stable solid-electrolyte interface (SEI) film at the lithium-electrolyte interface and the stability of MPIL electrolyte during cycling were investigated and discussed.

2. RESULTS AND DISCUSSION

The ionic liquid monomer, ATA, was prepared by the reaction of equimolar of 2-acrylamido-2-methyl-1-propanesulfonic acid (AMPS) and tris(dioxa-3,6-heptyl) amine (TDA) at room temperature. The chemical structure of ATA was confirmed by ¹H NMR and Fourier transform infrared (FTIR) spectra (Figures S1 and S3a, Supporting Information). The monomer ATA was then polymerized via free radical polymerization to give poly(ionic liquid), PATA, as shown in Scheme 1. The chemical structure of PATA was further confirmed by ¹H NMR and FTIR spectra (Figures S2 and S3b, Supporting Information). The obtained PATA has a molecular weight of 4.42×10^4 g mol⁻¹, with a molecular weight polydispersity of 1.73 as measured by gel permeation chromatography (GPC) (Figure S4, Supporting Information). The PATA is a viscous liquid at room temperature with a very low glass transition temperature of -51 °C measured by differential scanning calorimeter (DSC) and a thermal decomposition temperature

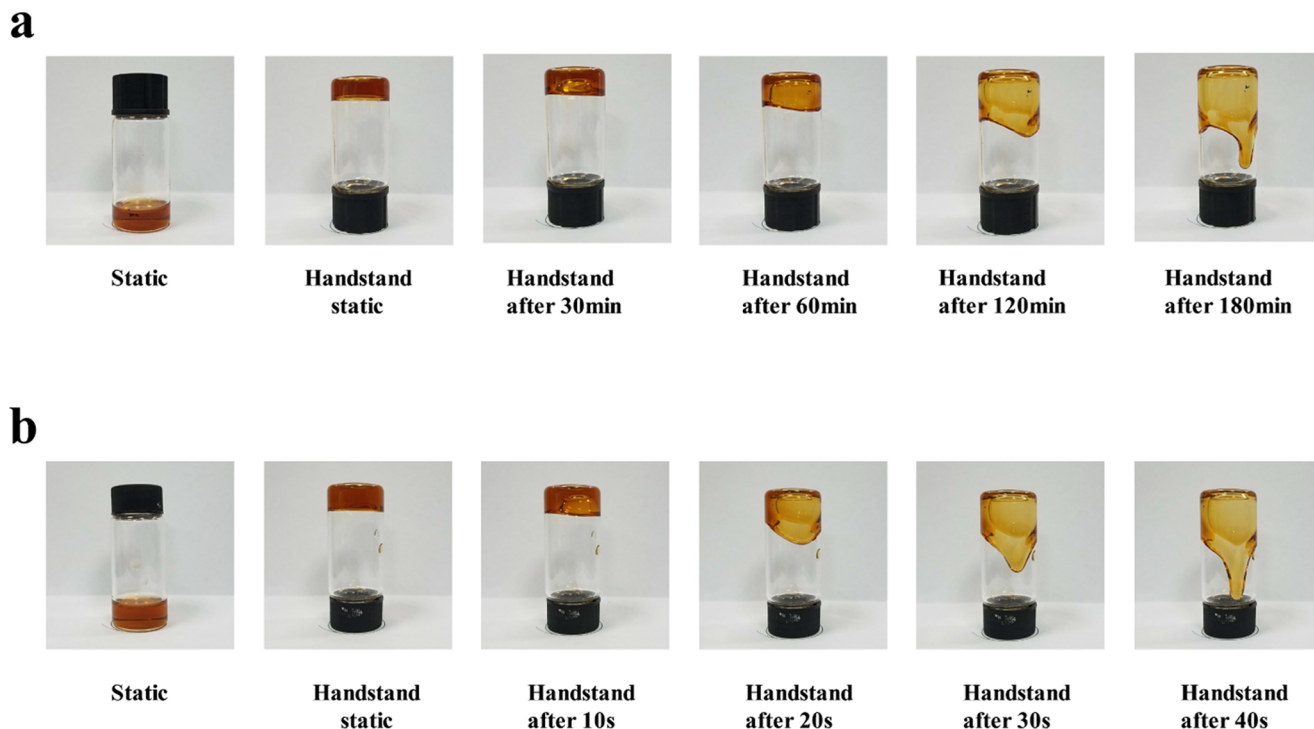


Figure 2. Flow behavior of (a) PATA and (b) MPIL at room temperature.

of 202.8 °C measured by thermogravimetric analysis (TGA) (**Figures S5 and S6**, Supporting Information).

To explore the usage of PATA as possible electrolyte for LIBs, we first investigated the electrochemical potential window and ionic conductivity of PATA by using an electrochemical workstation. The results indicated that PATA is stable up to the voltage of 4.62 V at 25 °C as shown in **Figure 1a**, which is much higher than the charge cutoff voltage of lithium–LiFePO₄ (LFP) battery, i.e., 3.8 V.²⁰ **Figure 1b** shows that the ionic conductivity of PATA with 0.1 M LiClO₄ increased with increase in temperature from 3.6×10^{-6} S cm⁻¹ at 25 °C to 1.37×10^{-4} S cm⁻¹ at 80 °C. It can be seen that the ionic conductivity of PATA at 25 °C is rather low to be used as an electrolyte in LIBs, which is due to the high viscosity of PATA, as shown in **Figure 2a**. Under the gravitation, the PATA hardly flowed in the initial 30 min and it took more than 180 min to flow down to the bottom of the glass bottle. To decrease the viscosity and hence enhance the ionic conductivity of PATA, we mixed small amount of PC (10 wt % of PATA) with PATA and 0.1 M LiClO₄, which was coded as MPIL. **Figure 2b** shows that the flow behavior of MPIL was significantly improved, and it only took 40 s to reach the bottom of the glass bottle. The amount of PC additive was optimized by measuring the ionic conductivity of PATA with 0.1 M LiClO₄ and various amount of PC and testing the cycling performance of LIBs with the corresponding mixtures as electrolytes (**Figure S7**, Supporting Information). The results of **Figure S7** indicate that the optimum amount of PC was 10 wt % of PATA. The MPIL shows the highest ionic conductivity and the LIB with MPIL as the electrolyte exhibits the best cycling performance. Furthermore, the fluidic behavior of MPIL is largely improved and the chemical potential window of MPIL is extended up to the voltage of 5.61 V at 25 °C (**Figure 1a**). The MPIL also exhibits a significantly enhanced ionic conductivity of 8.3×10^{-5} S cm⁻¹ at 25 °C (**Figure 1b**). Increasing the temperature to 60 °C can stabilize

the MPIL up to a voltage of 4.14 V with an ionic conductivity of 2.0×10^{-4} S cm⁻¹. The increase in electrochemical window of MPIL might be attributed to the following possible reasons. In the hybrid electrolyte, the poly(ionic liquid) has better mobility and activity, so it can unite with the surface active site of electrode more easily than that of pure PATA. The electrode was then passivated by the poly(ionic liquid) and the MPIL has a higher electrochemical window. On the other hand, the anodic stability window is limited by the irreversible oxidation of the salt anion.²¹ The addition of PC increases the activity ability of poly(ionic liquid) molecular chains and hence enhances the interaction between the –NH unit and SO₃[–] and ClO₄[–] anions, which might suppress the oxidation of these anions. Furthermore, the PC molecules are surrounded by large poly(ionic liquid) molecular chains, which also suppress the oxidation of PC. The depression of oxidation of salt anions and PC might cooperatively increase the electrochemical stability window of MPIL. The above results indicate that MPIL exhibits a wide potential window and a high ionic conductivity, rendering it suitable as an electrolyte for the lithium–LiFePO₄ battery.

Figure 3 shows the current variation in a [Li metal anode|MPIL electrolyte|Li metal cathode] cell as a function of time under a polarization voltage of 10 mV at 25 °C. The lithium-ion transference number (t_{Li^+}), which relates to the concentration polarization of electrolyte during the charging and discharging processes, can be then calculated as

$$t_{\text{Li}^+} = I_{ss} R_e^{ss} (\Delta V - I_0 R_0) / I_0 R_e^0 (\Delta V - I_{ss} R_f) \quad (1)$$

where I_0 is the initial current, I_{ss} is the steady current, R_0 is the initial lithium interfacial resistance, R_f is the final lithium interfacial resistance, R_e^0 is the initial electrolyte resistance, R_e^{ss} is the final electrolyte resistance, and ΔV is the polarization voltage of 10 mV. From **Figure 3**, t_{Li^+} is calculated to be 0.25 by using $I_0 = 8.8 \mu\text{A}$, $I_{ss} = 6.2 \mu\text{A}$, $R_e^0 = 186.7 \Omega$, $R_e^{ss} = 190 \Omega$, R_0

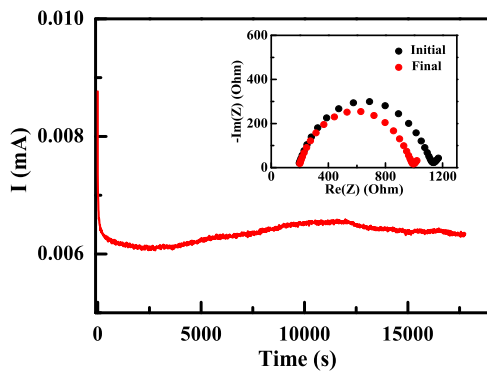


Figure 3. Current variation in a [Li metal anode|MPIL electrolyte|Li metal cathode] cell as a function of time under a polarization voltage of 10 mV at 25 °C. The inset shows the alternating current impedance spectra of the symmetrical cell before and after polarization.

$= 937.4 \Omega$, and $R_f = 797.4 \Omega$. The t_{Li^+} of 0.25 for MPIL is slightly higher than that of PEO-based composite solid polymer electrolytes (i.e., ~0.2) reported by Chen et al.²¹

The [Li metal anode|MPIL electrolyte|LiFePO₄-based cathode] batteries were then fabricated. The charge- and discharge-specific capacities of the batteries were first investigated at various current densities ranging from 0.1 to 5C ($1.0C = 0.12 \text{ mA cm}^{-2}$) under a voltage range of 2.7–3.8 V at 25 °C, as shown in Figure 4. Because of the Ohmic polarization, the charge and discharge capacities of the batteries gradually decreased with increasing current density. The charge and discharge capacities of the batteries at a current density of 0.1C were 130.4 and 130.5 mAh g⁻¹, respectively, about 76.7 and 76.8% of the theoretical value, i.e., 170 mAh g⁻¹. Furthermore, significant charge–discharge platforms were observed. At a current density of 1C, the charge-specific capacity only reduced to 75.6% of the original. Although increasing the current density to 5C resulted in a low discharge-specific capacity of only 29.6 mAh g⁻¹, the discharge-specific capacity of the battery recovered back to 127.3 mAh g⁻¹ when the current density turned back to 0.1C (Figure 4b).

Figure 5a shows the long-term cycling performance and the corresponding Coulombic efficiency of [Li metal anode|MPIL electrolyte|LiFePO₄-based cathode] batteries at various current densities at 25 °C during charge–discharge processes between 2.7 and 3.8 V. For the first cycle, the reversible discharge-specific capacities of the batteries were 137.4, 127, 112.6, and

110 mAh g⁻¹ at 0.1, 0.2, 0.5, and 1C, respectively. After running over 100 cycles, the discharge-specific capacities of the batteries were 127.4, 123.3, 119.2, and 116.3 mAh g⁻¹ at 0.1, 0.2, 0.5, and 1C, respectively, which indicated an excellent retention rate. The Coulombic efficiency was close to 100% at all current densities studied here, except for the first cycle. This outstanding cycling stability with a Coulombic efficiency of about 100% indicated that MPIL is an excellent electrolyte for lithium–LFP battery. These results are better than those reported by Lu et al.¹⁷ The reported Li/LiFePO₄ half-cell equipped with the PIL/30PC film shows an initial discharge-specific capacity of 120.4 mAh g⁻¹ with the corresponding Coulombic efficiency of 89.1% at 0.1C.¹⁷ However, the specific capacity of the battery decreases to 99.2 mAh g⁻¹ in the 30th cycle.¹⁷

We further tested the cycling performance of the batteries at elevated temperatures. Figure 5b shows that the [Li metal anode|MPIL electrolyte|LiFePO₄-based cathode] batteries also exhibited excellent cycling stability with a Coulombic efficiency of about 100% at 50 and 60 °C. The discharge-specific capacity and Coulombic efficiency for the first cycle increased with increasing temperature. However, the discharge-specific capacity of LIB running at 60 °C decreased slightly more than that at 50 °C because the lithium dendrites might grow faster at high temperature (see below).

The charge- and discharge-specific capacities of the batteries at 60 °C were also investigated at various current densities ranging from 0.1 to 5C under a voltage range of 2.7–3.8 V, as shown in Figure 6, which shows that the charge- and discharge-specific capacities of the battery at a current density of 0.1C at 60 °C were 154 and 144 mAh g⁻¹, respectively, higher than the corresponding values at 25 °C. The low charge–discharge platforms were observed, indicating that the cell polarization effect of LIBs was low. With the current density of 1C, the charge and discharge capacities of the battery at 60 °C were 128 and 125.8 mAh g⁻¹, respectively. Especially, when the current density was increased to 5C, the charge and discharge capacities of the battery at 60 °C were 105 and 100 mAh g⁻¹, respectively, more than 3 times the values at 25 °C (cf. Figure 4). Similarly, the discharge-specific capacity of the battery recovered back to 135 mAh g⁻¹ when the current density turned back from 5 to 0.1C (Figure 6b). These results further indicated that the LIBs using MPIL as electrolyte have better performance at higher temperature. These results are also better than those reported by Wang et al.,¹⁶ who reported that

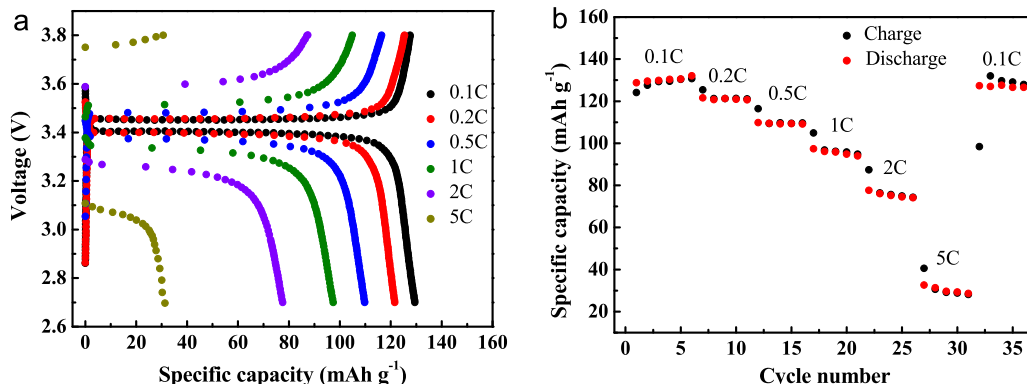


Figure 4. (a) Charge and discharge curves for [Li metal anode|MPIL electrolyte|LiFePO₄-based cathode] batteries measured at various current densities at 25 °C. (b) Rate performance of the batteries at 25 °C.

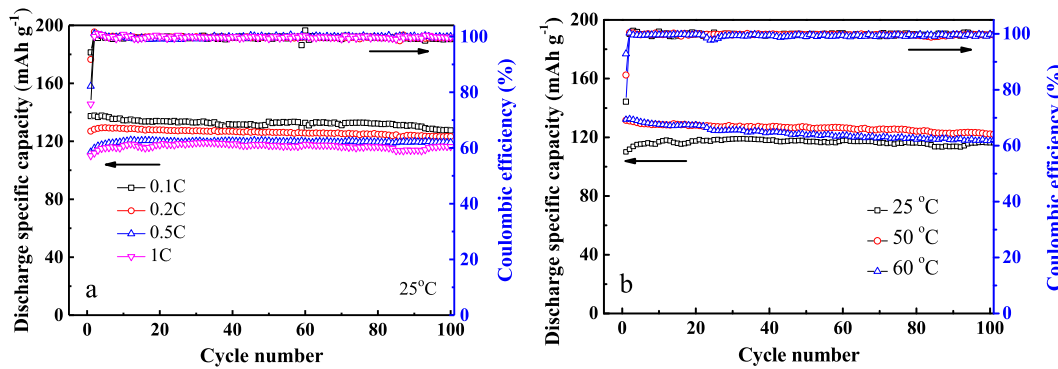


Figure 5. (a) Cycling stability of [Li metal anode|MPIL electrolyte|LiFePO₄-based cathode] batteries at various current densities at 25 °C. (b) Cycling stability of [Li metal anode|MPIL electrolyte|LiFePO₄-based cathode] batteries at the current density of 1C at 25, 50, and 60 °C, respectively.

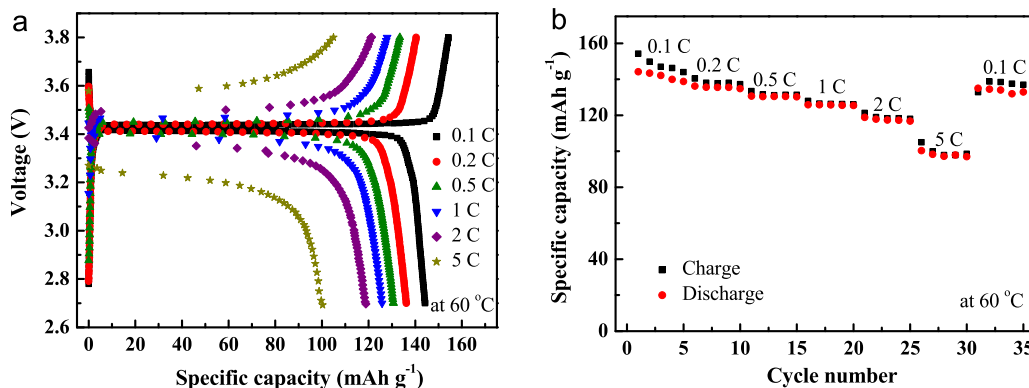


Figure 6. (a) Charge and discharge curves for [Li metal anode|MPIL electrolyte|LiFePO₄-based cathode] batteries measured at various current densities at 60 °C. (b) Rate performance of the batteries at 60 °C.

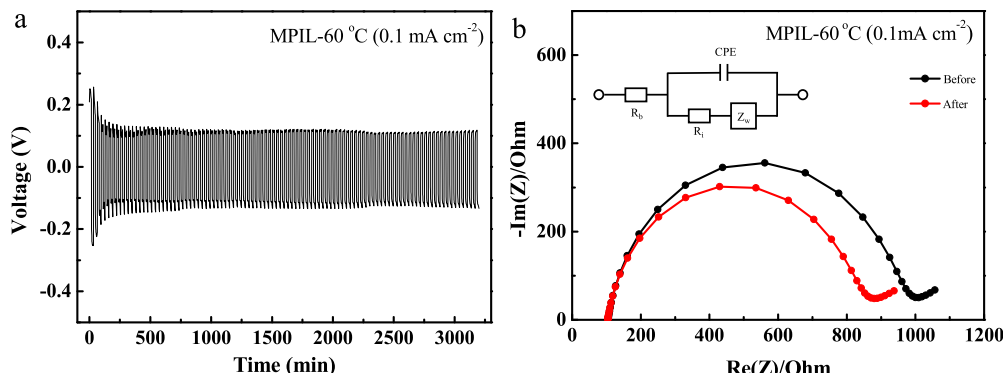


Figure 7. Li symmetrical cell (a) cycling and (b) EIS results of a cell containing MPIL electrolyte: 16 mm Li disk, constant current (0.1 mA cm⁻²) for 16 min, 100 cycles at 60 °C.

the PVIMTFSI-*co*-PPEGMA/LiTFSI-based LiFePO₄/Li battery shows the discharge-specific capacities of 136 and 70 mAh g⁻¹ at 0.1 and 1C, respectively, at 60 °C.

To gain a further understanding of the interfacial characteristics between MPIL/Li metal anode at high temperature, the charge-discharge cycling test of the lithium symmetrical cell at 60 °C was performed and the electrochemical impedance spectroscopy (EIS) before and after the test was also measured. Figure 7a shows the voltage-time profiles of the cell running for 100 cycles at 0.1 mA cm⁻² at 60 °C. As we can see, there are no sudden voltage fluctuations during the test, which indicates that the SEI film formed on the lithium-metal anode was stable and no short-circuit effect occurred. Figure

7b shows the impedance spectra of the lithium symmetrical cell before and after running for 100 cycles at 0.1 mA cm⁻² at 60 °C. And the modified Randles-type equivalent circuit obtained by computer simulations with the ZView software is also given as inset in Figure 7b. The intercept of the semicircle in the high-frequency region at the real axis is ascribed to the electrolyte bulk resistance (R_b), the diameter of the semicircle represents the interfacial resistance (R_i) of the MPIL/lithium-metal anode and the double-layer capacitor is replaced with a constant phase element, and Z_w is the Warburg diffusion. The R_b is determined to be 104.9 Ω before the cycle and 104 Ω after the cycle, respectively. The almost invariable R_b implies that the MPIL can be stable during the test. Furthermore, the

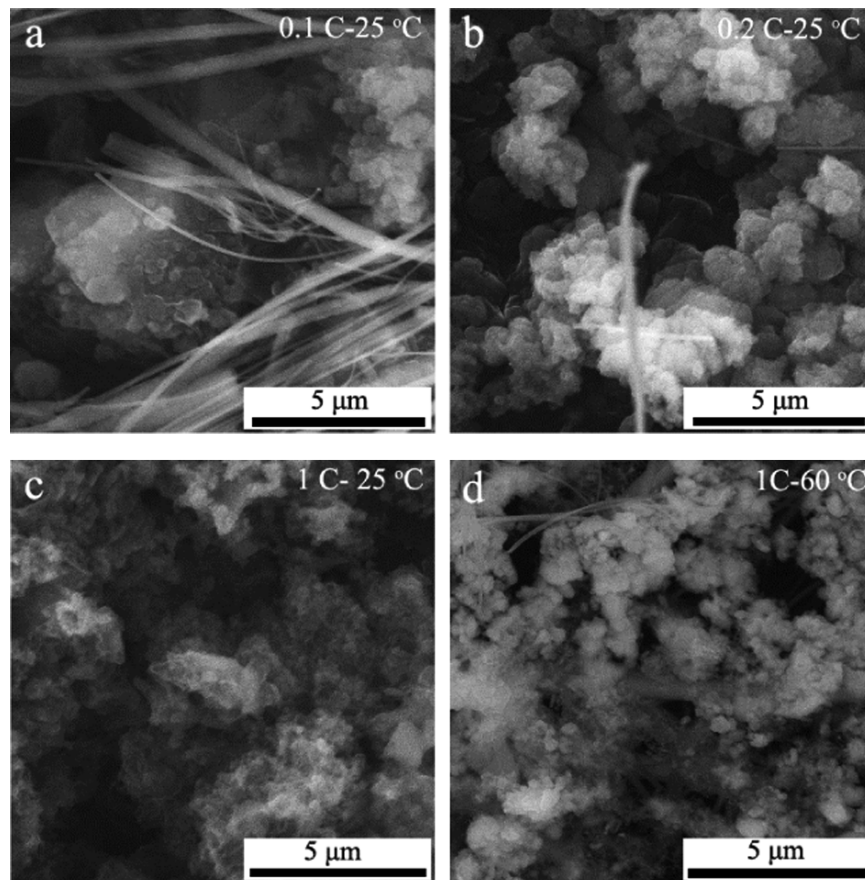


Figure 8. SEM images of the lithium slices of [Li metal anode|MPIL electrolyte|LiFePO₄-based cathode] batteries after 100 charge–discharge cycles at different current densities and different temperatures. (a) 0.1C and 25 °C, (b) 0.2C and 25 °C, (c) 1C and 25 °C, and (d) 1C and 60 °C.

R_i slightly reduces from 844 to 712 Ω after the cycling test, indicating the good compatibility between the MPIL and lithium metal.

The surface morphology of the lithium anode after 100 cycles under various testing conditions was observed by using scanning electron microscopy (SEM) to gain further understanding of the cycling behavior of the batteries. Figures 8 and S8 show that the morphology of lithium dendrite formed on the surface of lithium-metal electrode after 100 cycles. More lithium dendrites were observed at high C-rate. When increasing the temperature, the lithium dendrite begins to pierce the fiberglass diaphragm and large area lithium dendrites in fiberglass diaphragm can be seen at 1C and 60 °C (Figure 8d), which might result in the decrease in discharge-specific capacity of LIB running at 60 °C (cf. Figure 5b). Note that the white striped objects in the SEM images are the fibers from the fiberglass diaphragm.

The stability of the electrolyte during the charge and discharge process is very important for the usage of LIBs. The in situ differential electrochemical mass spectrometry (DEMS) measurement was further carried out to study the stability of MPIL in LIBs. Normally, the PC-based electrolyte and ether electrolyte tender to decompose and produce gas during the charge–discharge process of LIBs.^{22–24} Figure 9 shows that there is not significant CO₂ generation during the charge–discharge process, indicating that the MPIL electrolyte was electrochemically stable and did not decompose during the running of LIBs at the current density of 1C at 25 °C.

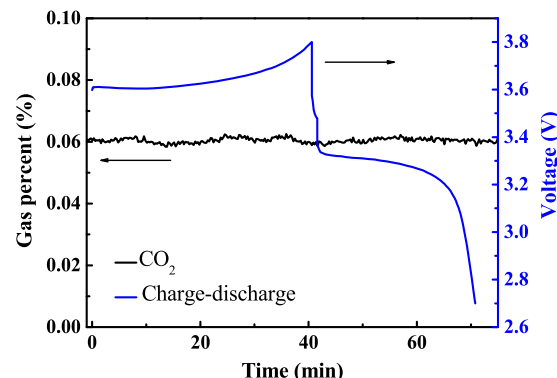


Figure 9. In situ DEMS result of the [Li metal anode|MPIL electrolyte|LiFePO₄-based cathode] battery running at the current density of 1C at 25 °C.

3. CONCLUSIONS

In summary, a novel PIL-based electrolyte, MPIL, by mixing a liquid-like poly(ionic liquid) with additives of 10 wt % propylene carbonate (PC) and 0.1 M LiClO₄, was fabricated and successfully applied in LIBs. The MPIL electrolyte exhibits a high ionic conductivity of 8.3×10^{-5} S cm⁻¹ at 25 °C or 2.0×10^{-4} S cm⁻¹ at 60 °C with a wide electrochemical potential window up to 5.61 V at 25 °C or 4.14 V at 60 °C. The Li/LiFePO₄ batteries with MPIL electrolyte achieve high capacity, outstanding cycling stability, and rate capability at 25 °C and improved performance at high temperature up to 60 °C, which are attributed to the formation of stable SEI film at the Li–

MPIL interface and the stability of MPIL during cycling. Such MPIL electrolyte might find wide potential application in LIBs with enhanced safety performance.

4. EXPERIMENTAL SECTION

4.1. Materials. 2-Acrylamido-2-methylpropanesulfonic acid (AMPS, J&K, 98%), lithium perchlorate (LiClO_4) (Aladdin, 99.99% metals basis), and tris(dioxa-3,6-heptyl)amine (TDA, J&K, 95%) were used without further purification. 2,2-Azobisisobutyronitrile (AIBN, Aladdin) was recrystallized and propylene carbonate (PC, Aladdin, 99.7%) was dried by 3A molecular sieve before use.

4.2. Synthesis of Ionic Liquid Monomer and Poly(ionic liquid). The ionic liquid monomer, ATA, was synthesized by adding 2.07 g AMPS (0.01 mol) and 3.23 g TDA (0.01 mol) into a round flask and stirring at room temperature for 12 h. The obtained monomer ATA (5.30 g, 0.01 mol) was then polymerized via free-radical polymerization with 0.0328 g AIBN (2×10^{-4} mol) as an initiator to give poly(ionic liquid), PATA. Briefly, 2% AIBN was added to ATA and polymerization was carried out at 80 °C for 8 h. After polymerization, the reaction mixture was dissolved in 10 mL acetone and then precipitated by 50 mL diethyl ether. The obtained PATA was yellow viscous liquid at the bottom of the glass beaker, which was carefully separated by a separating funnel, dried in vacuum at 80 °C for 24 h, and then kept in the glovebox for further uses.

4.3. Preparation of the Electrolyte and Cathode for Lithium-Ion Battery. The poly(ionic liquid) electrolyte used for lithium-ion battery in the present work consisted of 90 wt % PATA, 10 wt % PC, and 0.1 M LiClO_4 . The poly(ionic liquid)-based electrolyte was prepared in a glovebox by simple mixing of the three components and coded as MPIL for short. The cathode used herein was LiFePO_4 -based, which was prepared by mixing LiFePO_4 , poly(vinylidene fluoride), and carbon black in a weight ratio of 8:1:1 and aluminum foil as the current collector. The cathode was dried in vacuum at 80 °C for 24 h and then transferred into glovebox before use.

4.4. Characterizations. ^1H NMR spectrum was recorded on a Bruker 400 MHz spectrometer using dimethylsulfoxide- d_6 as solvent. The molecular weight and molecular weight distribution of PATA were measured by gel permeation chromatography (GPC) using a Water GPC and 0.1 M NaNO_3 aqueous solutions as the eluent with a flow rate of 0.80 mL min $^{-1}$ at 30 °C. The FTIR spectrum was recorded on a Vector 22 Bruker spectrometer. Thermogravimetric analysis (TGA) was carried out by using a TGA Q50 instrument with a heating rate of 10 °C min $^{-1}$ under N_2 atmosphere. The glass transition temperatures of ATA and PATA were measured by using a differential scanning calorimeter (DSC Q20) with a heating and cooling rate of 10 °C min $^{-1}$ under N_2 atmosphere. The temperature range for DSC measurement was set as -50–80 °C. The scanning electron microscopy (SEM) measurements were carried out on a Hitachi S-4800 SEM.

4.5. Electrochemical Performance Evaluation. The electrochemical stability and potential windows of PATA and MPIL were characterized by using a Bio-logic VMP3 multichannel potentiostatic–galvanostatic system. Linear sweep voltammetry measurements were carried out from the open-circuit voltage to 5 V (PATA) or 6 V (MPIL) vs Li/Li $^+$ with a potential scan rate of 1 mV s $^{-1}$. The conductivities of the PATA with 0.1 M LiClO_4 and MPIL at various temperatures were also characterized by the same instrument

with a 2-electrode Swagelok cell, in which a coin-like shaped membrane (1.13 cm 2 area and 0.044 cm thickness) was sandwiched between two stainless steel pistons. The conductivity (σ) was given as

$$\sigma = d/(R \times A) \quad (2)$$

where d is the thickness of the membrane (cm), A is the geometrical area of the membrane (cm 2), and R is the resistance calculated by the intercept of the curve with the real axis on the Nyquist plot (Ω).

The [Li metal anode|MPIL electrolyte|Li metal cathode] button cells were fabricated. A polarization voltage of 10 mV was given by the Bio-logic VMP3 multichannel potentiostatic–galvanostatic system for 5 h until the polarization current was stable. The impedance of the button cell was characterized by electrochemical impedance spectroscopy (EIS) scanning on the Bio-logic VMP3 multichannel potentiostatic–galvanostatic system with the frequency range from 100 kHz to 100 MHz with a perturbation amplitude of 5 mV.

The [Li metal anode|MPIL electrolyte| LiFePO_4 -based cathode] batteries were fabricated. The LiFePO_4 -based cathode was prepared as described above. The charge and discharge tests of the batteries at various current densities and temperature were conducted on LANHE system with a voltage range between 2.7 and 3.8 V. The in situ differential electrochemical mass spectrometry (DEMS) measurement was carried out by using a Hiden HPR-20 with 1.5 mL min $^{-1}$ Ar air flow between 2.7 and 3.8 V.

■ ASSOCIATED CONTENT

S Supporting Information

The Supporting Information is available free of charge on the ACS Publications website at DOI: [10.1021/acsomega.8b01539](https://doi.org/10.1021/acsomega.8b01539).

^1H NMR and FTIR spectra, TGA, and DSC curves of ionic liquid monomer ATA and poly(ionic liquid) PATA, GPC curve of PATA, digital photos of flow behavior of PATA and MPIL, temperature-dependent ionic conductivities of mixed electrolyte consisted of PATA, 0.1 M LiClO_4 and various amount of PC, cycling performance of [Li metal anode|mixed electrolyte LiFePO_4 -based cathode] batteries using different electrolyte, additional SEM images of the lithium slices (PDF)

■ AUTHOR INFORMATION

Corresponding Authors

*E-mail: duby@zju.edu.cn (B.D.).

*E-mail: zqpeng@ciac.ac.cn (Z.P.).

ORCID

Binyang Du: [0000-0002-5693-0325](https://orcid.org/0000-0002-5693-0325)

Zhangquan Peng: [0000-0002-4338-314X](https://orcid.org/0000-0002-4338-314X)

Notes

The authors declare no competing financial interest.

■ ACKNOWLEDGMENTS

The authors thank the National Natural Science Foundation of China (No. 21674097), the second level of 2016 Zhejiang Province 151 Talent Project, and Open Research Fund of State Key Laboratory of Polymer Physics and Chemistry (201601),

Changchun Institute of Applied Chemistry, Chinese Academy of Sciences for financial support.

■ REFERENCES

- (1) Yao, Y.; Qu, P.; Gan, X.; Huang, X.; Zhao, Q.; Liang, F. Preparation of porous-structured LiFePO₄/C composite by vacuum sintering for lithium-ion battery. *Ceram. Int.* **2016**, *42*, 18303–18311.
- (2) Naji, A.; Ghanbaja, J.; Willmann, P.; Billaud, D. New halogenated additives to propylene carbonate-based electrolytes for lithium-ion batteries. *Electrochim. Acta* **2000**, *45*, 1893–1899.
- (3) Tasaki, K.; Goldberg, A.; Winter, M. On the difference in cycling behaviors of lithium-ion battery cell between the ethylene carbonate- and propylene carbonate-based electrolytes. *Electrochim. Acta* **2011**, *56*, 10424–10435.
- (4) Kaneko, H.; Sekine, K.; Takamura, T. Power capability improvement of LiBOB/PC electrolyte for Li-ion batteries. *J. Power Sources* **2005**, *146*, 142–145.
- (5) Xiang, H.; Mei, D.; Yan, P.; Bhattacharya, P.; Burton, S. D.; et al. The Role of Cesium Cation in Controlling Interphasial Chemistry on Graphite Anode in Propylene Carbonate-Rich Electrolytes. *ACS Appl. Mater. Interfaces* **2015**, *7*, 20687–20695.
- (6) Chu, A. C.; Josefowicz, J. Y.; Far-rington, G. C. Electrochemistry of Highly Ordered Pyrolytic Graphite Surface Film Formation Observed by Atomic Force Microscopy. *J. Electrochem. Soc.* **1997**, *144*, 4161–4169.
- (7) Isken, P.; Winter, M.; Passerini, S.; Lex-Balducci, A. Methacrylate based gel polymer electrolyte for lithium-ion batteries. *J. Power Sources* **2013**, *225*, 157–162.
- (8) Kim, S. K.; Shin, B. J.; Kim, J. H.; Ahn, S.; Lee, S. Y. Nano-encapsulation of graphite-based anodes by a novel polymer electrolyte and its influence on C-rate performances of Li-ion batteries. *Electrochim. Commun.* **2008**, *10*, 1625–1628.
- (9) Kim, D. W.; Sun, Y. K. Electrochemical characterization of gel polymer electrolytes prepared with porous membranes. *J. Power Sources* **2001**, *102*, 41–45.
- (10) Huang, W.; Zhu, Z.; Wang, L.; Wang, S.; Li, H.; et al. Quasi-solid-state rechargeable lithium-ion batteries with a calix[4]quinone cathode and gel polymer electrolyte. *Angew. Chem., Int. Ed.* **2013**, *52*, 9162–9166.
- (11) Appetecchi, G. B.; Montanino, M.; Zane, D.; Carewska, M.; Alessandrini, F.; Passerini, S. Effect of the alkyl group on the synthesis and the electrochemical properties of -alkyl-methyl-pyrrolidinium bis(trifluoromethanesulfonyl)imide ionic liquids. *Electrochim. Acta* **2009**, *54*, 1325–1332.
- (12) Zhou, Q.; Henderson, W. A.; Appetecchi, G. B.; Montanino, M.; Passerini, S. Physical and Electrochemical Properties of N-Alkyl-N-methylpyrrolidinium Bis(fluorosulfonyl)imide Ionic Liquids: PY₁₃FSI and PY₁₄FSI. *J. Phys. Chem. B* **2008**, *112*, 13577–13580.
- (13) Kim, G.-T.; Jeong, S. S.; Xue, M. Z.; Balducci, A.; Winter, M.; et al. Development of ionic liquid-based lithium battery prototypes. *J. Power Sources* **2012**, *199*, 239–246.
- (14) Qian, W.; Texter, J.; Yan, F. Frontiers in poly(ionic liquid)s: syntheses and applications. *Chem. Soc. Rev.* **2017**, *46*, 1124–1159.
- (15) Xu, D.; Guo, J.; Yan, F. Porous ionic polymers: Design, synthesis, and applications. *Prog. Polym. Sci.* **2018**, *79*, 121–143.
- (16) Wang, A.; Liu, X.; Wang, S.; Chen, J.; Xu, H.; Xing, Q.; Zhang, L. Polymeric ionic liquid enhanced all-solid-state electrolyte membrane for high-performance lithium-ion batteries. *Electrochim. Acta* **2018**, *276*, 184–193.
- (17) Lu, F.; Gao, X.; Wu, A.; Sun, N.; Shi, L.; Zheng, L. Lithium-Containing Zwitterionic Poly(Ionic Liquid)s as Polymer Electrolytes for Lithium-Ion Batteries. *J. Phys. Chem. C* **2017**, *121*, 17756–17763.
- (18) Ricksaskoski, H. L.; Snow, A. W. Synthesis and electric field actuation of an ionic liquid polymer. *J. Am. Chem. Soc.* **2006**, *128*, 12402–12403.
- (19) Prescher, S.; Polzer, F.; Yang, Y.; Siebenbürger, M.; Ballauff, M.; Yuan, J. Polyelectrolyte as Solvent and Reaction Medium. *J. Am. Chem. Soc.* **2014**, *136*, 12–15.
- (20) Yang, C. C.; Hsu, Y. H.; Shih, J. Y.; Wu, Y. S.; Karuppiah, C.; et al. Preparation of 3D micro/mesoporous LiFePO₄ composite wrapping with porous graphene oxide for high-power lithium ion battery. *Electrochim. Acta* **2017**, *258*, 773–785.
- (21) Chen, B.; Huang, Z.; Chen, X.; Zhao, Y.; Xu, Q.; Long, P.; Chen, S.; Xu, X. A New Composite Solid Electrolyte PEO/Li₁₀GeP₂S₁₂/SN for all-solid-state lithium battery. *Electrochim. Acta* **2016**, *210*, 905–914.
- (22) Heine, J.; Hilbig, P.; Qi, X.; Niehoff, P.; Winter, M.; Bieker, P. Fluoroethylene Carbonate as Electrolyte Additive in Tetraethylene Glycol Dimethyl Ether Based Electrolytes for Application in Lithium Ion and Lithium Metal Batteries. *J. Electrochem. Soc.* **2015**, *162*, A1094–A1101.
- (23) Abe, K.; Yoshitake, H.; Kitakura, T.; Hattori, T.; Wang, H.; Yoshio, M. Additives-containing functional electrolytes for suppressing electrolyte decomposition in lithium-ion batteries. *Electrochim. Acta* **2004**, *49*, 4613–4622.
- (24) Xing, L.; Wang, C.; Li, W.; Xu, M.; Meng, X.; Zhao, S. Theoretical Insight into Oxidative Decomposition of Propylene Carbonate in the Lithium Ion Battery. *J. Phys. Chem. B* **2009**, *113*, 5181–5187.